Comparative Analysis of Wavelet-based Feature Extraction for Intramuscular EMG Signal Decomposition

Ghofrani Jahromi M.[1], Parsaei H.[1]*, Zamani A.[1], Dehbozorgi M.[1]

[1]Department of Medical Physics and Engineering, Shiraz University of Medical Sciences, Shiraz, Iran

ABSTRACT

Background: Electromyographic (EMG) signal decomposition is the process by which an EMG signal is decomposed into its constituent motor unit potential trains (MUPTs). A major step in EMG decomposition is feature extraction in which each detected motor unit potential (MUP) is represented by a feature vector. As with any other pattern recognition system, feature extraction has a significant impact on the performance of a decomposition system. EMG decomposition has been studied well and several systems were proposed, but feature extraction step has not been investigated in detail.

Objective: Several EMG signals were generated using a physiologically-based EMG signal simulation algorithm. For each signal, the firing patterns of motor units (MUs) provided by the simulator were used to extract MUPs of each MU. For feature extraction, different wavelet families including Daubechies (db), Symlets, Coiflets, bi-orthogonal, reverse bi-orthogonal and discrete Meyer were investigated. Moreover, the possibility of reducing the dimensionality of MUP feature vector is explored in this work. The MUPs represented using wavelet-domain features are transformed into a new coordinate system using Principal Component Analysis (PCA). The features were evaluated regarding their capability in discriminating MUPs of individual MUs.

Results: Extensive studies on different mother wavelet functions revealed that db2, coif1, sym5, bior2.2, bior4.4, and rbior2.2 are the best ones in differentiating MUPs of different MUs. The best results were achieved at the 4th detail coefficient. Overall, rbior2.2 outperformed all wavelet functions studied; nevertheless for EMG signals composed of more than 12 MUPTs, syms5 wavelet function is the best function. Applying PCA slightly enhanced the results.

Keywords

Electromyographic signal, EMG decomposition, Decomposability index, Feature extraction, Motor Unit Potential Classification, Wavelet Function, Wavelet Transform

Introduction

An electromyographic (EMG) signal detected during a muscle contraction, reflects the electrical activity of the motor units (MUs) recruited during this contraction. In other words, an EMG signal is the sequence of voltages detected from a contracting muscle over time. The potentials are detected in the voltage field generated by the active muscle fibers of a contracting muscle. Surface and needle electrodes such as concentric, monopolar as well as single fiber needle

*Corresponding author: H. Parsaei
Department of Medical Physics and Engineering, Shiraz University of Medical Sciences, Shiraz, Iran
E-mail: hparsaei@sums.ac.ir

Received: 16 February 2016
Accepted: 9 March 2016

electrodes are the common types of electrodes that are used to detect EMG signals. The detected signal using electrodes is, in fact, the superposition of the motor unit potential trains (MUPTs) and background noise. The signals acquired using surface electrodes are known as surface EMG signals and those recorded with indwelling electrodes are called needle EMG signals.

Surface electrodes are easy to use, noninvasive and do not cause pain. However, the signals detected using these electrodes (i.e., surface EMG signals) do not contain detailed information about deep muscles, mainly due to the low pass filtering characteristics of the volume conduction properties of the overlying muscles as well as other subcutaneous tissues. Needle electrodes, on the other hand, provide selective recordings as they can be inserted in precise locations and have small recording areas. For diagnostic purposes, it is useful to obtain detailed temporal and spatial information about the fibers of an MU, thus indwelling electrodes inserted into a muscle are used to acquire EMG signals.

The characteristics of an EMG signal recorded during a muscle contraction depend on several factors such as the level of muscle contraction, the shape and size of the electrode used, the position and orientation of the electrode relative to the muscle fibers of the active MUs, the anatomical and physiological features of the muscle and the age and state of health or fatigue of the muscle. Consequently, an EMG signal reveals valuable information for physiological investigation along with clinical examinations to diagnose, treat as well as to manage neuromuscular disorders. EMG signal decomposition, the procedure of resolving an EMG signal into its component MUPTs, is an efficient method for retrieving such information. The main target of EMG signal decomposition is extracting the firing pattern, MUP template along with MUP shape stability of each active MU which contributed significantly to the EMG signal being analyzed.

Various EMG decomposition systems and algorithms have been proposed. Parsaei et al. provided an extensive review of the algorithms developed for the decomposition of intramuscular EMG signals in [1]. Several techniques, from signal acquisition to MUP grouping, as well as numerous types of electrodes, both single and multi-channel, along with different signal processing, clustering and supervised classification techniques have been utilized in developing automated or semi-automated EMG decomposition algorithms [1-20], but the main focuses of researchers was clustering and classifying steps. Each of these systems uses their own feature extraction, classification and clustering techniques. The performance of clustering and classification algorithms in grouping MUPs have been studied and reported; however, the performance and discrimination power of the features have not been studied yet. Nevertheless, in an EMG decomposition system, like any pattern recognition system, the features used for representing examples and patterns play an important role in the overall performance of the system. Therefore, a cross comparison of the feature extraction methods used in EMG signal decomposition can assist in choosing the best features for representing MUPs and ultimately may improve EMG decomposition results. The purpose of this work is to address this issue. Specifically, our target is to explore the potential of employing the coefficients from discrete wavelet transform of MUPs as a feature extraction method in order to achieve higher MUPT separability, and hence a greater EMG decomposition precision.

EMG Signal Decomposition

EMG signal decomposition is the procedure of partitioning a raw EMG signal into its constituent MUPTs. An EMG decomposition system could consist of four major steps: signal preprocessing, MUP detection, feature extraction along with clustering and supervised clas-

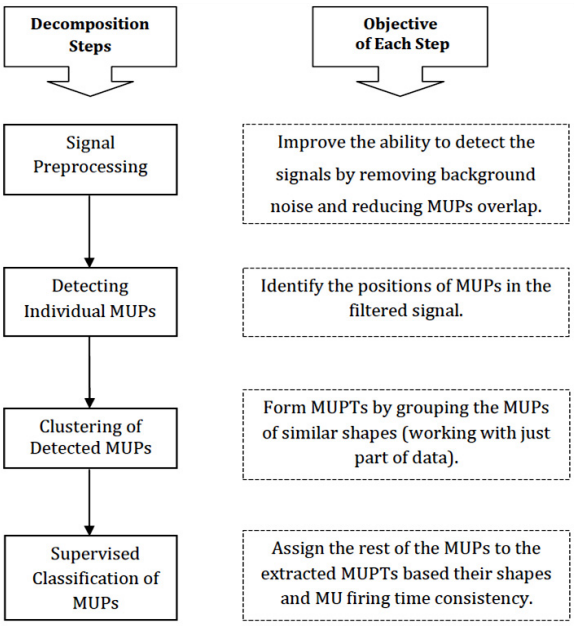

Figure 1: Main steps of an EMG decomposition system along with the objective of each step [9]

sification of detected MUPs. Figure 1 demonstrates a short description of the objective of each step. A short description of each step is presented under sub-sections 2.1 to 2.4, respectively.

Signal Preprocessing

As with any signal analysis method, the initial phase in decomposing of an acquired EMG signal is removing, as much as possible, the background noise contaminating a signal. The noise includes instrumentation noise and artifacts. A band-pass filter with adequate cut-off frequencies can remove low-frequency baseline drifts and also high-frequency noise. In addition to improving signal-to-noise ratio (SNR), an efficient filtering technique can enhance the contrast between the MUPs of different MUs. This technique can make the clustering easier [2, 3]. In general, band-pass filters or low-pass difference (LPD) filters are the most widely used filters in this step [1-3].

Signal Segmentation and MUP Detection

The objective of this step is to partition an EMG signal into segments containing possible MUPs. The threshold crossing technique usually is used for this purpose. In this method, the raw or filtered signal is inspected for negative or positive peaks which exceed a specified threshold. These peaks indicate candidate MUP positions. A window centered at each identified peak is then applied to the signal and the data points that falls in the window are stored as a MUP. The threshold can also be chosen manually or adaptively. An option for setting the threshold value is the root mean square (RMS) value of the signal multiplied by a constant [4-8]. Figure 2 shows an example of a simple MUP detection technique. In

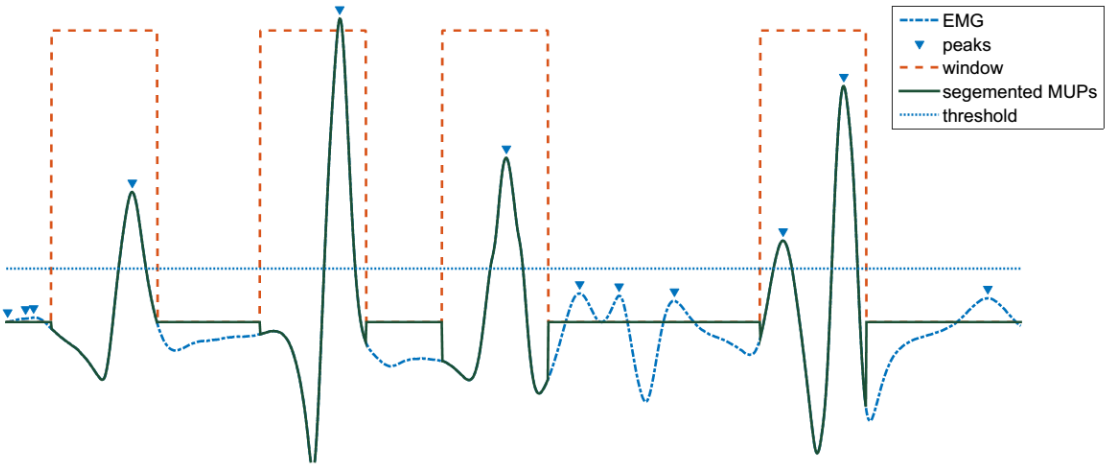

Figure 2: Segmentation of a signal into MUPs

Figure 3 a shimmer plot of the MUPs detected in an EMG signal is illustrated.

Feature Extraction

In this step, each MUP which is detected in the previous step is represented by a set of features called feature vector. The feature vector used to represent each MUP has a significant role in the overall accuracy and the speed of a decomposition algorithm. Ideally, a feature vector should be comprised of a minimum number of uncorrelated features that are easy to compute, capable of discriminating between different classes and minimally sensitive to contaminating noise [10].

To date, different types of features have been used to represent detected MUPs in EMG decomposition which can be categorized as: the MUP time samples, first or second derivatives of time samples [4, 5, 7, 9, 11–20], morphology of MUPs [8, 21–25], Fourier transform or power spectrum coefficients [2, 26, 27] and Wavelet coefficients [28-33]; see [1] for more information.

Different Wavelet decomposition techniques, in terms of mother wavelet and decomposition level, have been used for EMG decomposition [3, 28-34]. EMG-LODEC system [29] based on the works of Zennaro [28] and Wellig [30] uses Daubechies wavelet coefficients as features. They showed both analytically and experimentally that lower bands of wavelet coefficients exhibit lower shimmer, and hence they are more appropriate to represent MUPs in a new feature space. They have reported that regarding accuracy, their system outperforms the method of Gut and Moschytz [7]. Yamada et al. [31], compared the accuracy of a decomposition system using either wavelet coefficients or their principal components. After applying complete linkage clustering on both feature vectors, the ones enhanced by principal component analysis (PCA) improved decomposition accuracy. Ren et al. [32] have used and compared four different feature sets in the minimum spanning tree clustering algorithm: original data, the waveform morphological features, wavelet coefficients and a fuzzy-based optimal wavelet packet features [34]. A fuzzy C-means (FCM) classification method is used to refine the results. Accuracy and processing time are compared for all the methods as well as refinements they have introduced. The best choice was using the optimal wavelet packet features including FCM-optimized classification. Rasheed et al. [33] used both first-order discrete derivative along with wavelet-domain features. Daubechies-4 mother wavelet was chosen and a 6-level dis-

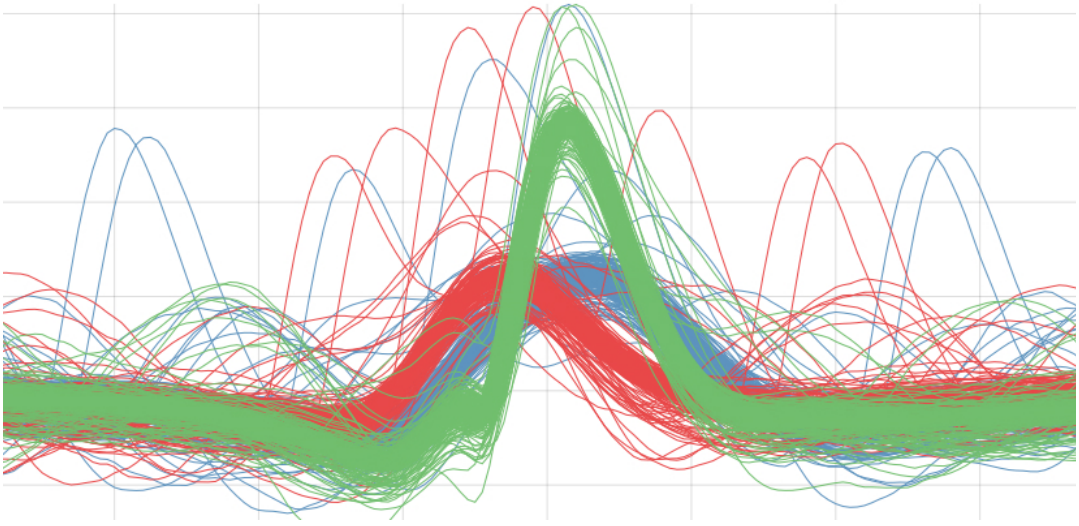

Figure 3: A shimmer plot of the MUPs detected in an EMG signal

crete wavelet transform was executed. Only detail coefficients at levels 4 to 6 were fed to their hybrid classifiers.

Clustering and Classification

In machine learning and statistics, classification is the problem of assigning a label to a new observation, according to a model which is extracted from a training set of data containing observations whose category or membership is already known. On the other hand, clustering is the duty of categorizing a set of objects so that the objects in the same group, which are called a cluster, share similar features. The EMG decomposition by its nature is a clustering task by which similar MUPs are sorted into several groups such that each group represents an MUPT. Grouping MUPs in EMG decomposition process could be completed using just a clustering algorithm or a clustering as well as a classification algorithm [1]. Common clustering techniques employed in EMG decomposition consist of single or complete linkage, minimum spanning tree, self-organizing neural networks, fuzzy c-means and k-means. In addition, template matching, certainty-based methods and artificial neural networks are the most widely used methods for classification. See [1] for a list of methods using specific clustering or classification algorithms.

If a full or complete decomposition is required, in addition to the four steps discussed, the employed decomposition system contains another step in which superimposed MUPs are resolved into their constituent MUPs [4, 15], [22, 35-40]. However, for applications in which only mean MU firing rate and MU firing rate variability are of interest, such as clinical applications, resolving superimposed MUPs is not necessary because the desired MU firing parameters can be estimated from incomplete discharge patterns [1, 10].

Methods

One objective in this research was to find the most suitable wavelet for repressing MUPs in EMG signal decomposition. This section expresses the details of the steps towards this aim.

Data

Several simulated EMG signals were used in this study. Forty four EMG signals were generated using physiologically-based EMG signal simulation algorithm developed by Hamilton-Wright and Stashuk [41]. In the presented model, primarily, the physical layout of a muscle together with the electrode position is considered. Then according to a defined value for maximum volume contraction, a number of motor units required to obtain the EMG signal are recruited. Therefore, this intramuscular EMG signal simulator enables us to create intramuscular EMG signals with different complexities represented by the average number of MUP patterns per second (pps), the numbers of active motor unit (adjusted by setting the level of MVC), the amount of MUP shape variability represented by jitter and/or inter–discharge intervals (IDI) variability. The simulator, for each generated EMG signal, provides the discharge patterns for each MU contributed significantly to the EMG signal. These MU discharge patterns were used as a reference. Given the firing pattern of each MU in a given EMG signal, its MUP are extracted by placing a window of 161 samples centered at each firing time. This window represents MUP intervals of 5.152 ms at a sampling rate of 31.25 kHz.

Discrete Wavelet Transform for EMG Decomposition

Transformations, in general, are applied to a raw signal in order to obtain further information from that signal, which is not readily available in the raw signal (i.e., time –domain). Wavelet transform (WT) of a signal is an efficient method for representing both time and frequency information of a given signal. In fact, the WT of a signal provides a two-dimensional time-frequency representa-

tion of the signal. Although there are several methods such as Wigner-ville distribution and short–time Fourier transforms for time-frequency representation of a signal, it has been shown that the WT outperforms such traditional methods as it transforms the signals with a flexible resolution in both time and frequency domains. Specifically, the WT is a useful tool for processing non-stationary and time-varying signals processing particularly the biomedical signals.

The WT method is categorized into two types: continuous wavelet transforms (CWT) and discrete wavelet transforms (DWT). Continuous wavelet transform (CWT) of a square integrable signal, x(t), is defined by equation (1).

$$CWT(a,b) \triangleq \int_{-\infty}^{\infty} x(t) \frac{1}{\sqrt{|a|}} \psi^* \left(\frac{t-b}{a} \right) dt \qquad (1)$$

where the real numbers a and b are called scale (or dilation) and translation parameters, respectively, and $\psi(t)$ is the mother wavelet. In fact, the CWT illustrates how well a wavelet function correlates with the mother wavelet $\psi(t)$.

Discrete wavelet transform (DWT) of a signal with length N is attained by choosing $a=2^j$ and $b=k2^j$ and considering CWT as the convolution of $x(t)$ and $h(t)=\frac{1}{\sqrt{2^j}}\psi(-\frac{t}{2^j})$. However, it is more common to view DWT from a filter bank perspective. By successively passing the given signal $x[n]$ through a series of low-pass and high-pass filters, wavelet coefficients are computed. Passing the samples through a low pass filter results in approximation coefficients, and filtering the signal with a high pass filter provides detailed coefficients. Mathematically, DWT can be expressed as:

$$s[n] = \sum_{k=-\infty}^{\infty} x[k] h[2n-k]$$

$$d[n] = \sum_{k=-\infty}^{\infty} x[k] g[2n-k]$$

Where $h[n]$ represents the impulse response of low-pass filter, $S[n]$ is approximation coefficient, $g[n]$ represents that of the impulse response of high-pass filter and $d[n]$ stands for detailed coefficients. This process is continued to further extract wavelet coefficients. Figure 4 illustrates how an input signal $x[n]$ is passed through three successive approximation and detail filters. The outputs contain the contents of the signal at different frequency sub-bands. The tree is known as a filter bank. If the detail coefficients decompose further wavelet packet decomposition is achieved.

CWT and DWT have several advantages and disadvantages. CWT is more efficient and reliable than DWT, as it maintains all information without down-sampling. However, the computational complexity of CWT is higher than that of DWT. In other words, DWT is faster than CWT. The issue with CWT is that it is highly redundant.

During analyzing a signal using WT method, two major factors should be considered: the type of wavelet and the level of decomposition. Different types of wavelets have different time-frequency structures.

One objective of this study was to find the most suitable wavelet for repressing MUPs in EMG signal decomposition. To achieve this purpose, different wavelet families including Daubechies (db), Symlets, Coiflets, bi-orthogonal, reverse bi-orthogonal and discrete Meyer have been investigated. Table 1 lists different types of wavelet functions with their families examined in this study. The wavelet-domain features are extracted by taking the DWT of each detected MUP. By decomposing a given MUP using DWT, the MUP pattern feature vector would be the concatenation of the detail coefficients at all scale levels and the approximation coefficients at the last scale level. Mathematically, the wavelet-domain feature vector of an MUP obtained by applying an M–level of DWT (i.e., $V^{(M)}$)) can be represented as $v^{(M)}=(s_M, d_M, d_{M-1}, d_{M-2}, \ldots, d_2, d_1)$ where s_M stands for approximation coefficients and d_M

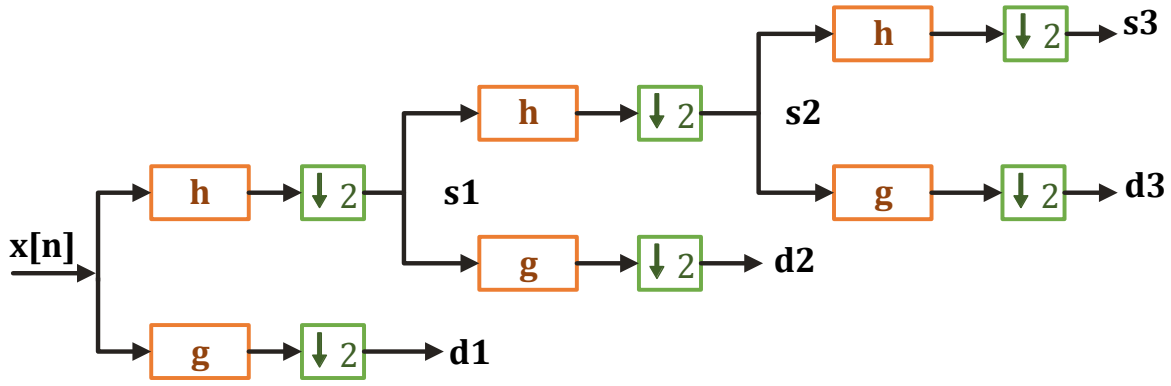

Figure 4: A 3-level discrete wavelet decomposition of a signal x[n]. SM represents approximation coefficients and dM symbolizes detailed coefficients obtained at level M

Table 1: Wavelet functions used in this work

Wavelet Families	Function in MATLAB
Daubechies	db1, db2, db3, db4, db5, db6, db7, db8, db9, db10, db11, db12, db13, db14, db15
Symlets	sym2, sym3, sym4, sym5, sym6, sym7, sym8
Coiflets	coif1, coif2, coif3, coif4, coif5
Biorthogonal	bior1.1, bior1.3, bior1.5, bior2.2, bior2.4, bior2.6, bior2.8, bior3.1, bior3.3, bior3.5, bior3.7, bior3.9, bior4.4, bior5.5, bior6.8
Reverse Biorthogonal	rbio1.1, rbio1.3, rbio1.5, rbio2.2, rbio2.4, rbio2.6, rbio2.8, rbio3.1, rbio3.3, rbio3.5, rbio3.7, rbio3.9, rbio4.4, rbio5.5, rbio6.8
Discrete Meyer	dmey

stands for detailed coefficients estimated at M^{th} level.

The possibility of reducing the dimensionality of the MUP feature vector is explored in this work. The MUPs represented using wavelet-domain features are transformed to a new coordinate system using PCA [42]. PCA is an unsupervised method that tries to seek a set of new orthogonal features each of which is a linear combination of the original features. The criterion of orthogonality ensures that PCA provides new features with the least amount of redundant information [43]. In this system, each coordinate is responsible for a section of the given data variance according to its order, which means, the first coordinate forms the most significant part, the second one owns the second most considerable section and so forth. The first K principal components, which are responsible for a particular part, e.g, β%, of the variance in the data are the most impressive specifications in certain data. The value of K is the dimension of the feature space used to represent the MUPs of a given MUPT. The optimized value for the parameter β was figured out empirically.

Evaluation Criteria

In EMG signal decomposition, features used to represent each MUP should be capable of discriminating between MUPs of distinct MUs. In this research, to quantify the discriminative power of the wavelet-domain features, two evaluating criteria were used: Decomposability Index and Predictive Accuracy.

Decomposability Index (DI) is an index proposed by Parsaei and Stashuk [20] to measure the decomposability of a given EMG. In fact, this index measures how distinguishable the MUPs of an MU are from those of other MUs

in an EMG signal. See reference [9] or [20] for the details of the calculation of DI for an EMG signal.

Predictive accuracy of a classifier is a regular basis to assess the quality of features used to represent patterns. In this method, the accuracy of a predetermined learning algorithm over a different set of features is estimated, and the set that provides the highest accuracy is selected as the best feature set. The main idea here is that the more powerful the features, the higher the accuracy of the classifiers will be. In this work, a kNN classifier with k=5 is chosen for all features. In addition, cross validation was used to find an optimum value for k.

Results and Discussion

Table 2 (presented in pages 374 and 375) gives the DI values for all mother wavelets studied in this research. The results are summarized in Figures 5-7. Figure 5 presents DI values and Figure 6 depicts predictive accuracy rates of the best mother wavelets versus the number of MUs contributing in the generation of each EMG signal. Figure 7 shows the box plots. The presented results were produced using M = 4 (a 4–level decomposition in DWT) and β=95%. These user-defined parameters were determined empirically using some simulated EMG signals used in this work.

The results suggest that mother wavelets *db2*, *coif1*, *sym5*, *bior2.2*, *bior4.4* and *rbior2.2* have a better capability in differentiating between MUPs created by different MUs. In addition, applying PCA to the wavelet–domain feature values slightly improved the discrimination of MUPs. However, when using PCA, one should consider its computational complexity. Moreover, combining coefficients from different sub-bands or applying PCA on a batch of sub-bands did not improve the values of DI. Among all the wavelet functions studied in this work (listed in Table 1), the reverse biorthogonal 2.2 (*rbior2.2*) outperformed other wavelet functions.

It can be revealed from Figures 5 and 7 that in general as the number of MUs contributed in EMG signal increases, the decomposition complexity of the signal increases mainly because when the number of active MUs in-

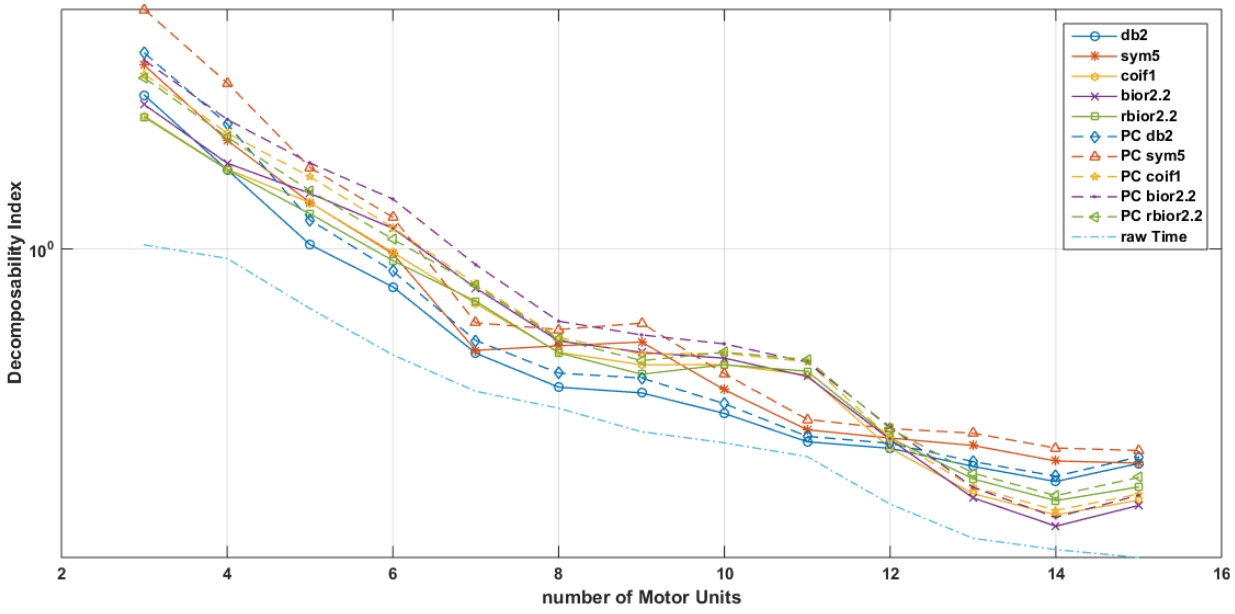

Figure 5: Decomposability Index achieved using different wavelet functions

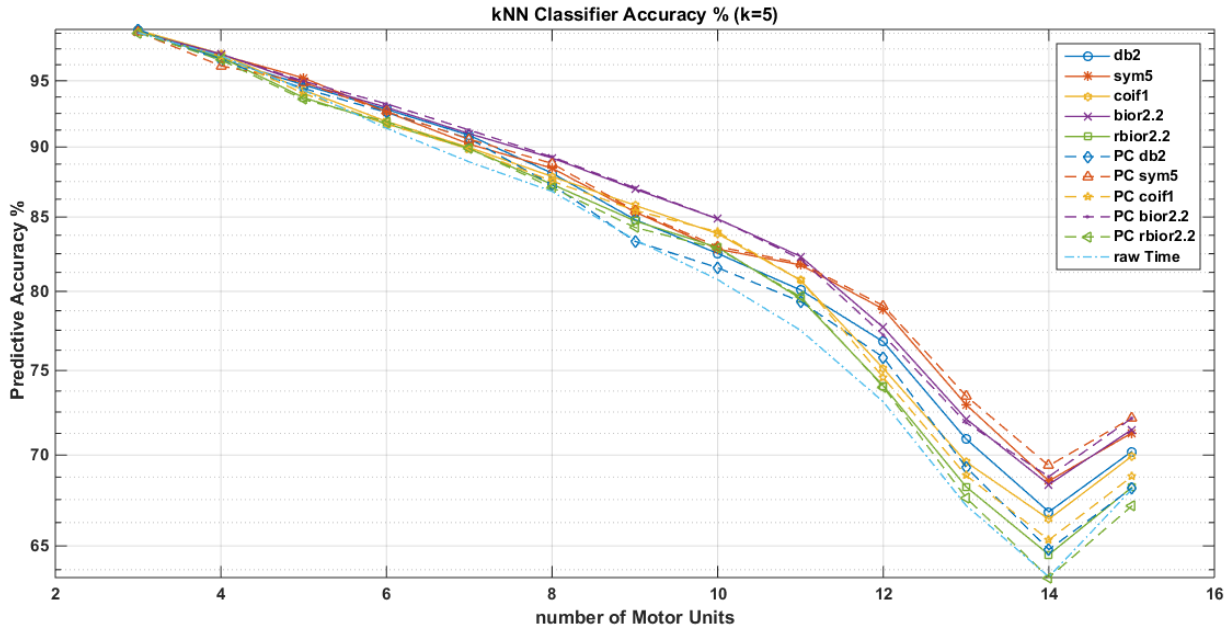

Figure 6: kNN classification accuracy rate, (k=5) achieved using different wavelet functions

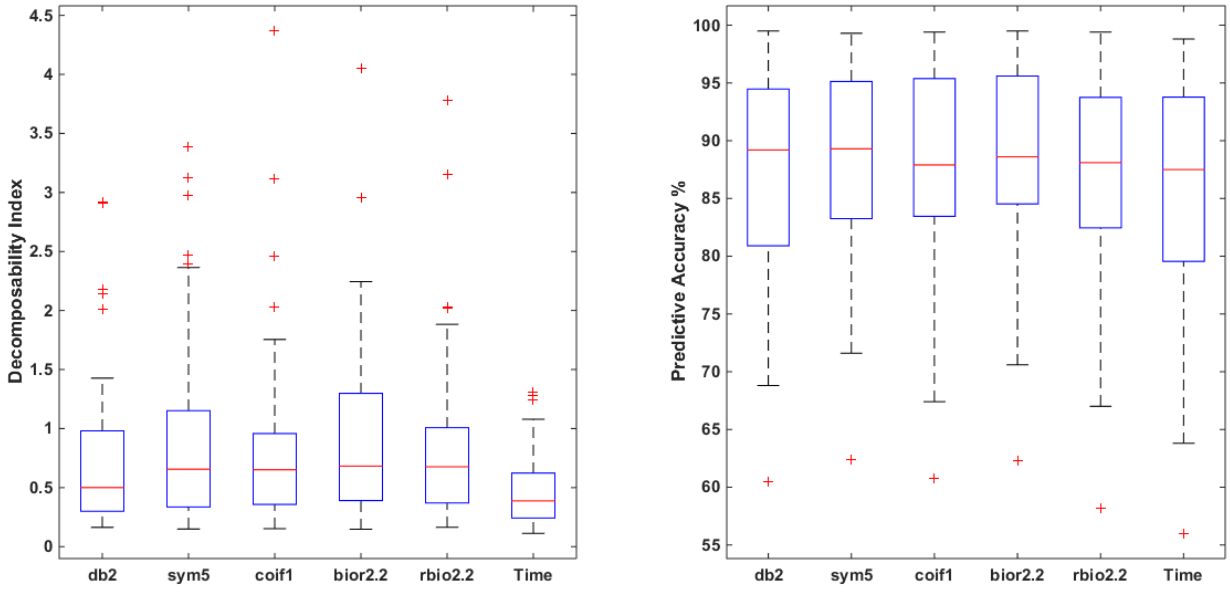

Figure 7: Decomposability index (left) and classification accuracy (right) achieved using selected wavelet function and time samples

Table 2: Decomposability Indices, Median [25th Percentile, 75th Percentile] obtained using different DWT-based feature extraction methods. For the sake of comparison, these values for time samples are 0.39 [0.24 0.62].

Wavelet Function	Approx. 4	PCA Approx. 4	Detail 4	PCA Detail 4	Detail 3	PCA Detail 3	Detail 2	PCA Detail 2	Detail 1	PCA Detail 1
db1	0.32 [0.19 0.55]	0.32 [0.20 0.59]	0.41 [0.29 0.58]	0.41 [0.30 0.64]	0.59 [0.33 0.85]	0.70 [0.35 0.99]	0.58 [0.34 1.08]	0.67 [0.36 1.28]	0.55 [0.33 1.01]	0.55 [0.33 1.05]
db2	0.29 [0.18 0.40]	0.31 [0.19 0.41]	0.50 [0.30 0.98]	0.54 [0.32 1.07]	0.57 [0.38 1.19]	0.63 [0.42 1.37]	0.37 [0.27 0.84]	0.41 [0.30 0.95]	0.12 [0.07 0.24]	0.12 [0.07 0.24]
db3	0.26 [0.16 0.37]	0.26 [0.16 0.39]	0.54 [0.31 0.81]	0.59 [0.33 0.91]	0.42 [0.20 0.73]	0.44 [0.20 0.84]	0.20 [0.09 0.42]	0.21 [0.10 0.47]	0.02 [0.01 0.04]	0.02 [0.01 0.04]
db4	0.24 [0.14 0.36]	0.25 [0.14 0.38]	0.35 [0.20 0.60]	0.37 [0.20 0.65]	0.35 [0.17 0.64]	0.38 [0.18 0.70]	0.08 [0.04 0.19]	0.08 [0.04 0.21]	0.01 [0.01 0.01]	0.01 [0.01 0.01]
db5	0.21 [0.13 0.27]	0.21 [0.13 0.29]	0.51 [0.25 0.98]	0.58 [0.27 1.12]	0.18 [0.06 0.31]	0.19 [0.06 0.33]	0.06 [0.03 0.13]	0.07 [0.03 0.13]	0.00 [0.00 0.01]	0.00 [0.00 0.01]
db6	0.19 [0.12 0.28]	0.20 [0.12 0.30]	0.35 [0.18 0.56]	0.37 [0.18 0.61]	0.25 [0.13 0.59]	0.27 [0.14 0.68]	0.05 [0.02 0.10]	0.06 [0.02 0.11]	0.00 [0.00 0.00]	0.00 [0.00 0.00]
db7	0.17 [0.11 0.28]	0.17 [0.11 0.28]	0.24 [0.13 0.42]	0.26 [0.14 0.45]	0.14 [0.06 0.26]	0.15 [0.06 0.28]	0.03 [0.01 0.06]	0.03 [0.01 0.07]	0.00 [0.00 0.00]	0.00 [0.00 0.00]
db8	0.16 [0.10 0.22]	0.16 [0.10 0.22]	0.24 [0.13 0.45]	0.25 [0.13 0.49]	0.27 [0.11 0.47]	0.29 [0.11 0.52]	0.02 [0.01 0.04]	0.02 [0.01 0.04]	0.00 [0.00 0.00]	0.00 [0.00 0.00]
db9	0.15 [0.09 0.23]	0.15 [0.10 0.24]	0.27 [0.15 0.54]	0.29 [0.15 0.60]	0.12 [0.06 0.26]	0.13 [0.06 0.29]	0.03 [0.01 0.06]	0.03 [0.01 0.06]	0.00 [0.00 0.00]	0.00 [0.00 0.00]
db10	0.14 [0.09 0.23]	0.14 [0.09 0.23]	0.32 [0.18 0.56]	0.34 [0.18 0.61]	0.17 [0.08 0.35]	0.18 [0.09 0.38]	0.01 [0.01 0.03]	0.01 [0.01 0.03]	0.00 [0.00 0.00]	0.00 [0.00 0.00]
db11	0.14 [0.08 0.19]	0.13 [0.08 0.19]	0.47 [0.20 0.82]	0.51 [0.21 0.94]	0.13 [0.08 0.32]	0.13 [0.08 0.35]	0.01 [0.01 0.03]	0.01 [0.01 0.03]	0.00 [0.00 0.00]	0.00 [0.00 0.00]
db12	0.13 [0.08 0.20]	0.12 [0.08 0.20]	0.45 [0.23 0.88]	0.48 [0.24 0.97]	0.16 [0.06 0.32]	0.17 [0.06 0.35]	0.02 [0.01 0.05]	0.02 [0.01 0.05]	0.00 [0.00 0.00]	0.00 [0.00 0.00]
db13	0.12 [0.07 0.18]	0.12 [0.07 0.18]	0.45 [0.27 0.86]	0.48 [0.28 0.96]	0.15 [0.09 0.34]	0.16 [0.09 0.38]	0.01 [0.01 0.03]	0.01 [0.01 0.03]	0.00 [0.00 0.00]	0.00 [0.00 0.00]
db14	0.11 [0.07 0.16]	0.11 [0.07 0.16]	0.42 [0.24 0.74]	0.46 [0.25 0.84]	0.12 [0.05 0.24]	0.12 [0.05 0.26]	0.01 [0.01 0.02]	0.01 [0.01 0.02]	0.00 [0.00 0.00]	0.00 [0.00 0.00]
db15	0.11 [0.07 0.17]	0.11 [0.07 0.17]	0.27 [0.13 0.50]	0.28 [0.13 0.53]	0.15 [0.07 0.31]	0.16 [0.07 0.34]	0.02 [0.01 0.04]	0.02 [0.01 0.04]	0.00 [0.00 0.00]	0.00 [0.00 0.00]
coif1	0.26 [0.16 0.35]	0.25 [0.16 0.37]	0.65 [0.36 0.96]	0.71 [0.39 1.06]	0.46 [0.30 0.99]	0.51 [0.33 1.11]	0.29 [0.20 0.67]	0.31 [0.21 0.74]	0.11 [0.07 0.23]	0.11 [0.07 0.23]
coif2	0.19 [0.11 0.30]	0.20 [0.12 0.31]	0.31 [0.21 0.67]	0.33 [0.22 0.73]	0.19 [0.10 0.42]	0.19 [0.10 0.46]	0.05 [0.02 0.13]	0.06 [0.03 0.14]	0.01 [0.00 0.01]	0.01 [0.00 0.01]
coif3	0.15 [0.09 0.23]	0.16 [0.09 0.23]	0.18 [0.10 0.28]	0.18 [0.10 0.30]	0.07 [0.03 0.15]	0.07 [0.03 0.16]	0.02 [0.01 0.07]	0.03 [0.01 0.07]	0.00 [0.00 0.00]	0.00 [0.00 0.00]
coif4	0.13 [0.08 0.18]	0.13 [0.08 0.19]	0.13 [0.07 0.26]	0.13 [0.07 0.27]	0.10 [0.05 0.21]	0.10 [0.05 0.23]	0.01 [0.01 0.04]	0.01 [0.01 0.05]	0.00 [0.00 0.00]	0.00 [0.00 0.00]
coif5	0.11 [0.07 0.17]	0.11 [0.07 0.16]	0.23 [0.12 0.34]	0.24 [0.11 0.36]	0.07 [0.03 0.16]	0.08 [0.03 0.17]	0.01 [0.01 0.03]	0.01 [0.01 0.03]	0.00 [0.00 0.00]	0.00 [0.00 0.00]
sym2	0.29 [0.18 0.40]	0.31 [0.19 0.41]	0.50 [0.30 0.98]	0.54 [0.32 1.07]	0.57 [0.38 1.19]	0.63 [0.42 1.37]	0.37 [0.27 0.84]	0.41 [0.30 0.95]	0.12 [0.07 0.24]	0.12 [0.07 0.24]
sym3	0.26 [0.16 0.37]	0.26 [0.16 0.39]	0.54 [0.31 0.81]	0.59 [0.33 0.91]	0.42 [0.20 0.73]	0.44 [0.20 0.84]	0.20 [0.09 0.42]	0.21 [0.10 0.47]	0.02 [0.01 0.04]	0.02 [0.01 0.04]
sym4	0.23 [0.14 0.34]	0.23 [0.14 0.36]	0.53 [0.31 0.82]	0.57 [0.32 0.97]	0.29 [0.11 0.51]	0.32 [0.12 0.55]	0.07 [0.03 0.14]	0.07 [0.03 0.15]	0.01 [0.00 0.01]	0.01 [0.00 0.01]
sym5	0.21 [0.13 0.27]	0.21 [0.13 0.29]	0.66 [0.34 1.15]	0.72 [0.35 1.35]	0.16 [0.10 0.39]	0.16 [0.10 0.42]	0.03 [0.02 0.07]	0.03 [0.02 0.07]	0.00 [0.00 0.01]	0.00 [0.00 0.01]
sym6	0.19 [0.12 0.30]	0.20 [0.12 0.30]	0.42 [0.23 0.75]	0.46 [0.25 0.83]	0.18 [0.07 0.31]	0.19 [0.07 0.33]	0.03 [0.02 0.06]	0.03 [0.02 0.07]	0.00 [0.00 0.01]	0.00 [0.00 0.01]
sym7	0.18 [0.11 0.25]	0.18 [0.11 0.25]	0.35 [0.23 0.63]	0.38 [0.24 0.74]	0.09 [0.04 0.18]	0.08 [0.04 0.19]	0.04 [0.01 0.08]	0.04 [0.02 0.08]	0.00 [0.00 0.00]	0.00 [0.00 0.00]
sym8	0.17 [0.10 0.26]	0.17 [0.10 0.26]	0.22 [0.13 0.43]	0.24 [0.14 0.46]	0.11 [0.06 0.25]	0.11 [0.06 0.27]	0.02 [0.01 0.05]	0.02 [0.01 0.06]	0.00 [0.00 0.00]	0.00 [0.00 0.00]
dmey	0.08 [0.06 0.12]	0.07 [0.05 0.11]	0.09 [0.06 0.19]	0.09 [0.06 0.19]	0.08 [0.05 0.13]	0.08 [0.04 0.13]	0.02 [0.01 0.03]	0.02 [0.01 0.03]	0.00 [0.00 0.00]	0.00 [0.00 0.00]

Wavelet Function	Approx. 4	PCA Approx. 4	Detail 4	PCA Detail 4	Detail 3	PCA Detail 3	Detail 2	PCA Detail 2	Detail 1	PCA Detail 1
bior1.1	0.32 [0.19 0.55]	0.33 [0.20 0.58]	0.41 [0.29 0.58]	0.45 [0.30 0.60]	0.59 [0.33 0.85]	0.67 [0.35 0.96]	0.58 [0.34 1.08]	0.66 [0.36 1.25]	0.55 [0.33 1.01]	0.55 [0.33 1.01]
bior1.3	0.28 [0.16 0.42]	0.29 [0.17 0.44]	0.38 [0.27 0.65]	0.39 [0.30 0.70]	0.64 [0.39 1.03]	0.73 [0.43 1.25]	0.59 [0.35 1.02]	0.67 [0.38 1.17]	0.54 [0.32 0.98]	0.54 [0.32 0.98]
bior1.5	0.23 [0.14 0.32]	0.23 [0.14 0.33]	0.47 [0.31 0.78]	0.50 [0.33 0.81]	0.57 [0.36 1.07]	0.64 [0.39 1.20]	0.52 [0.30 0.94]	0.58 [0.32 1.05]	0.53 [0.31 0.96]	0.53 [0.31 0.96]
bior2.2	0.29 [0.18 0.41]	0.31 [0.19 0.43]	0.68 [0.39 1.30]	0.75 [0.43 1.60]	0.40 [0.25 0.80]	0.43 [0.26 0.92]	0.17 [0.11 0.39]	0.18 [0.12 0.42]	0.09 [0.05 0.18]	0.09 [0.05 0.18]
bior2.4	0.25 [0.15 0.40]	0.26 [0.16 0.42]	0.54 [0.34 0.92]	0.59 [0.38 1.04]	0.26 [0.14 0.42]	0.28 [0.15 0.46]	0.15 [0.10 0.29]	0.16 [0.10 0.32]	0.08 [0.05 0.18]	0.08 [0.05 0.18]
bior2.6	0.22 [0.13 0.37]	0.23 [0.14 0.39]	0.30 [0.19 0.69]	0.31 [0.20 0.74]	0.21 [0.11 0.40]	0.22 [0.12 0.43]	0.14 [0.08 0.31]	0.15 [0.09 0.34]	0.08 [0.05 0.18]	0.08 [0.05 0.18]
bior2.8	0.21 [0.12 0.32]	0.21 [0.13 0.33]	0.13 [0.08 0.27]	0.14 [0.08 0.28]	0.17 [0.11 0.33]	0.17 [0.12 0.35]	0.14 [0.09 0.27]	0.15 [0.09 0.29]	0.08 [0.05 0.17]	0.08 [0.05 0.17]
bior3.1	0.41 [0.25 0.77]	0.45 [0.26 0.85]	0.39 [0.32 0.83]	0.41 [0.34 1.03]	0.37 [0.17 0.70]	0.40 [0.18 0.78]	0.03 [0.01 0.06]	0.04 [0.02 0.07]	0.01 [0.01 0.02]	0.01 [0.01 0.02]
bior3.3	0.33 [0.20 0.52]	0.35 [0.20 0.55]	0.37 [0.27 0.96]	0.42 [0.29 1.09]	0.14 [0.06 0.26]	0.15 [0.06 0.28]	0.03 [0.02 0.06]	0.03 [0.02 0.07]	0.01 [0.01 0.02]	0.01 [0.01 0.02]
bior3.5	0.28 [0.17 0.43]	0.29 [0.18 0.46]	0.28 [0.15 0.55]	0.30 [0.15 0.61]	0.09 [0.04 0.15]	0.10 [0.04 0.16]	0.03 [0.01 0.05]	0.03 [0.01 0.05]	0.01 [0.01 0.02]	0.01 [0.01 0.02]
bior3.7	0.24 [0.16 0.33]	0.25 [0.16 0.35]	0.19 [0.11 0.44]	0.19 [0.12 0.48]	0.06 [0.03 0.16]	0.07 [0.03 0.17]	0.02 [0.02 0.06]	0.03 [0.02 0.06]	0.01 [0.01 0.02]	0.01 [0.01 0.02]
bior3.9	0.22 [0.13 0.31]	0.22 [0.14 0.32]	0.11 [0.05 0.19]	0.12 [0.05 0.21]	0.13 [0.05 0.27]	0.14 [0.05 0.29]	0.02 [0.01 0.04]	0.03 [0.01 0.05]	0.01 [0.01 0.02]	0.01 [0.01 0.02]
bior4.4	0.20 [0.12 0.29]	0.20 [0.12 0.31]	0.58 [0.31 0.97]	0.64 [0.33 1.10]	0.18 [0.07 0.31]	0.19 [0.07 0.33]	0.05 [0.02 0.09]	0.05 [0.02 0.10]	0.01 [0.00 0.01]	0.01 [0.00 0.01]
bior5.5	0.14 [0.09 0.22]	0.14 [0.09 0.22]	0.47 [0.24 0.80]	0.52 [0.25 0.91]	0.12 [0.06 0.28]	0.13 [0.06 0.30]	0.03 [0.01 0.06]	0.03 [0.01 0.06]	0.00 [0.00 0.00]	0.00 [0.00 0.00]
bior6.8	0.16 [0.09 0.25]	0.16 [0.10 0.26]	0.15 [0.09 0.31]	0.15 [0.10 0.33]	0.10 [0.05 0.18]	0.11 [0.05 0.19]	0.03 [0.01 0.05]	0.03 [0.01 0.06]	0.00 [0.00 0.00]	0.00 [0.00 0.00]
rbio1.1	0.32 [0.19 0.55]	0.33 [0.20 0.58]	0.41 [0.29 0.58]	0.45 [0.30 0.60]	0.59 [0.33 0.85]	0.67 [0.35 0.96]	0.58 [0.34 1.08]	0.66 [0.36 1.25]	0.55 [0.33 1.01]	0.55 [0.33 1.01]
rbio1.3	0.26 [0.15 0.39]	0.27 [0.15 0.41]	0.36 [0.22 0.59]	0.38 [0.23 0.63]	0.46 [0.29 0.94]	0.52 [0.32 1.08]	0.19 [0.08 0.39]	0.20 [0.09 0.43]	0.02 [0.01 0.04]	0.02 [0.01 0.04]
rbio1.5	0.19 [0.12 0.27]	0.19 [0.12 0.28]	0.44 [0.30 0.75]	0.47 [0.32 0.83]	0.20 [0.13 0.48]	0.22 [0.13 0.52]	0.03 [0.01 0.07]	0.03 [0.01 0.07]	0.00 [0.00 0.01]	0.00 [0.00 0.01]
rbio2.2	0.22 [0.14 0.30]	0.23 [0.14 0.31]	0.68 [0.37 1.01]	0.74 [0.40 1.13]	0.55 [0.38 1.05]	0.61 [0.41 1.21]	0.42 [0.29 0.92]	0.46 [0.32 1.03]	0.15 [0.09 0.31]	0.15 [0.09 0.31]
rbio2.4	0.17 [0.11 0.24]	0.17 [0.11 0.24]	0.55 [0.33 0.97]	0.60 [0.34 1.04]	0.40 [0.17 0.63]	0.42 [0.19 0.72]	0.10 [0.04 0.21]	0.10 [0.04 0.23]	0.01 [0.01 0.01]	0.01 [0.01 0.01]
rbio2.6	0.14 [0.09 0.21]	0.14 [0.09 0.20]	0.37 [0.26 0.75]	0.37 [0.27 0.79]	0.12 [0.06 0.27]	0.13 [0.05 0.29]	0.05 [0.02 0.11]	0.05 [0.02 0.12]	0.00 [0.00 0.01]	0.00 [0.00 0.01]
rbio2.8	0.12 [0.07 0.18]	0.12 [0.07 0.17]	0.24 [0.14 0.41]	0.25 [0.15 0.42]	0.08 [0.04 0.17]	0.09 [0.04 0.18]	0.04 [0.02 0.08]	0.04 [0.02 0.09]	0.00 [0.00 0.00]	0.00 [0.00 0.00]
rbio3.1	0.25 [0.15 0.35]	0.26 [0.16 0.36]	0.44 [0.27 0.64]	0.47 [0.28 0.67]	0.57 [0.35 0.91]	0.61 [0.37 1.05]	0.63 [0.36 1.09]	0.71 [0.38 1.26]	0.57 [0.34 1.05]	0.57 [0.34 1.05]
rbio3.3	0.18 [0.11 0.24]	0.18 [0.11 0.25]	0.46 [0.33 0.82]	0.50 [0.35 0.90]	0.62 [0.42 1.18]	0.71 [0.48 1.36]	0.39 [0.26 0.82]	0.43 [0.28 0.95]	0.03 [0.02 0.09]	0.03 [0.02 0.09]
rbio3.5	0.14 [0.09 0.19]	0.15 [0.09 0.19]	0.42 [0.31 0.91]	0.45 [0.32 1.05]	0.33 [0.21 0.76]	0.35 [0.23 0.84]	0.10 [0.04 0.20]	0.10 [0.04 0.21]	0.01 [0.00 0.01]	0.01 [0.00 0.01]
rbio3.7	0.12 [0.07 0.16]	0.12 [0.07 0.17]	0.42 [0.26 1.00]	0.44 [0.27 1.25]	0.07 [0.04 0.15]	0.07 [0.03 0.16]	0.11 [0.05 0.21]	0.12 [0.05 0.22]	0.00 [0.00 0.00]	0.00 [0.00 0.00]
rbio3.9	0.10 [0.07 0.15]	0.10 [0.06 0.15]	0.41 [0.21 0.82]	0.44 [0.22 0.91]	0.12 [0.05 0.25]	0.12 [0.05 0.26]	0.03 [0.02 0.10]	0.04 [0.02 0.11]	0.00 [0.00 0.00]	0.00 [0.00 0.00]
rbio4.4	0.21 [0.13 0.32]	0.21 [0.14 0.32]	0.55 [0.32 0.95]	0.60 [0.35 1.04]	0.32 [0.15 0.58]	0.34 [0.16 0.63]	0.09 [0.04 0.20]	0.10 [0.04 0.22]	0.01 [0.01 0.02]	0.01 [0.01 0.02]
rbio5.5	0.24 [0.15 0.40]	0.26 [0.16 0.41]	0.47 [0.26 0.81]	0.50 [0.27 0.88]	0.21 [0.10 0.46]	0.22 [0.11 0.50]	0.08 [0.04 0.17]	0.08 [0.04 0.18]	0.01 [0.01 0.02]	0.01 [0.01 0.02]
rbio6.8	0.15 [0.09 0.23]	0.15 [0.09 0.23]	0.20 [0.12 0.37]	0.21 [0.12 0.40]	0.09 [0.04 0.18]	0.09 [0.04 0.19]	0.04 [0.02 0.07]	0.04 [0.02 0.08]	0.00 [0.00 0.00]	0.00 [0.00 0.00]

creases, the number of superimposed MUPs and ultimately the variability of samples in each class (i.e., MUPT) increases. Likewise, the effectiveness of feature extraction methods studied in discriminating MUPs reduces, for such hard-to decompose signals syms5 wavelet function performed better than the other functions nevertheless *rbior2.2* outperformed all wavelet functions on average. It should be noted that there are several other factors such MU firing pattern, MUP shape variability, SNR of a signal that affect the decomposability of a given EMG signal; here we did not investigate the performance of the feature extraction methods for each of these parameters individually. Nevertheless, the DI used in this work considers MUP shape variably and SNR implicitly [20].

Conclusion

EMG signal decomposition is a common approach to exploit inherent information in an EMG signal. Feature vector used to represent MUPs have a significant role in the precision of decomposition system. In this research, different wavelet families including Daubechies, Symlets, Coiflets, bi-orthogonal, reverse bi-orthogonal and discrete Meyer have been studied to find the most suitable wavelet for repressing MUPs in EMG decomposition. Results revealed that MUs were most separable after imposing a 4-level DWT and considering the detail-4 coefficients while using the wavelets *db2*, *coif1*, *sym5*, *bior2.2*, *bior4.4* or *rbior2.2*. Applying PCA slightly improved the results.

Acknowledgment

The paper has been extracted from parts of the M.Sc. thesis by Mohsen Ghofrani Jahromi supported by the Research Council of Shiraz University of Medical Sciences (93-01-01-9029).

Conflict of Interest

None

References

1. Parsaei H, Stashuk DW, Rasheed S, Farkas C, Hamilton-Wright A. Intramuscular EMG signal decomposition. *Crit Rev Biomed Eng*. 2010;**38**:435-65. doi.org/10.1615/CritRevBiomedEng.v38.i5.20. PubMed PMID: 21175408.
2. McGill KC, Cummins KL, Dorfman LJ. Automatic decomposition of the clinical electromyogram. *Biomedical Engineering, IEEE Transactions on*. 1985;(7):470-7.
3. McGill KC, Lateva ZC, Marateb HR. EMGLAB: an interactive EMG decomposition program. *J Neurosci Methods*. 2005;**149**:121-33. doi.org/10.1016/j.jneumeth.2005.05.015. PubMed PMID: 16026846.
4. Katsis CD, Goletsis Y, Likas A, Fotiadis DI, Sarmas I. A novel method for automated EMG decomposition and MUAP classification. *Artif Intell Med*. 2006;**37**:55-64. doi.org/10.1016/j.artmed.2005.09.002. PubMed PMID: 16377160.
5. Nikolic M, Krarup C. EMGTools, an adaptive and versatile tool for detailed EMG analysis. *IEEE Trans Biomed Eng*. 2011;**58**:2707-18. doi.org/10.1109/TBME.2010.2064773. PubMed PMID: 20699205.
6. Christodoulou CI, Pattichis CS. Unsupervided pattern recognition for the classification of EMG signals. *IEEE Trans Biomed Eng*. 1999;**46**:169-78. doi.org/10.1109/10.740879. PubMed PMID: 9932338.
7. Gut R, Moschytz GS. High-precision EMG signal decomposition using communication techniques. *Signal Processing, IEEE Transactions on*. 2000;**48**:2487-94. doi.org/10.1109/78.863051.
8. Nandedkar SD, Barkhaus PE, Charles A. Multimotor unit action potential analysis (MMA). *Muscle Nerve*. 1995;**18**:1155-66. doi.org/10.1002/mus.880181012. PubMed PMID: 7659110.
9. Parsaei H. EMG signal decomposition using motor unit potential train validity .[Thesis]. University of Waterloo: Waterloo, Ontario, Canada; 2011.
10. Stashuk D. EMG signal decomposition: how can it be accomplished and used? *J Electromyogr Kinesiol*. 2001;**11**:151-73. doi.org/10.1016/S1050-6411(00)00050-X. PubMed PMID: 11335147.
11. Stashuk DW. Decomposition and quantitative analysis of clinical electromyographic signals. *Med Eng Phys*. 1999;**21**:389-404. doi.org/10.1016/S1350-4533(99)00064-8 . PubMed PMID: 10624736.
12. Hassoun MH, Wang C, Spitzer AR. NNERVE: neural network extraction of repetitive vectors for electromyography--Part I: Algorithm.

IEEE Trans Biomed Eng. 1994;**41**:1039-52. doi.org/10.1109/10.335842. PubMed PMID: 8001993.

13. Nikolic M, Sorensen J, Dahl K, Krarup C, editors. Detailed analysis of motor unit activity. Engineering in Medicine and Biology Society, 1997. Proceedings of the 19th Annual International Conference of the IEEE; 1997: IEEE. doi.org/10.1109/iembs.1997.756600.
14. Christodoulou CI, Pattichis CS, editors. A new technique for the classification and decomposition of EMG signals. Neural Networks, 1995. Proceedings., IEEE International Conference on; 1995: IEEE. doi.org/10.1109/icnn.1995.487720.
15. Haas W, Meyer M. An automatic EMG decomposition system for routine clinical examination and clinical research-ARTMUP. Amsterdam, the Netherlands: Elsevier Science; 1989. p. 67-81.
16. Koch V, Loeliger H-A, editors. EMG signal decomposition by loopy belief propagation. Acoustics, Speech, and Signal Processing, 2005 Proceedings(ICASSP'05) IEEE International Conference on; 2005. doi: 10.1109/icassp.2005.1416324*.
17. Nawab SH, Wotiz RP, De Luca CJ. Multi-receiver precision decomposition of intramuscular EMG signals. Conf Proc IEEE Eng Med Biol Soc. 2006;1:1252-5. doi.org/10.1109/iembs.2006.260320. PubMed PMID: 17945629.
18. Nawab SH, Wotiz RP, De Luca CJ. Decomposition of indwelling EMG signals. *J Appl Physiol* (1985). 2008;**105**:700-10. doi.org/10.1152/japplphysiol.00170.2007. PubMed PMID: 18483170. PubMed PMCID: 2519944.
19. Erim Z, Lin W. Decomposition of intramuscular EMG signals using a heuristic fuzzy expert system. *IEEE Trans Biomed Eng*. 2008;**55**:2180-9. doi.org/10.1109/TBME.2008.923915. PubMed PMID: 18713687.
20. Parsaei H, Stashuk DW. EMG signal decomposition using motor unit potential train validity. *IEEE Trans Neural Syst Rehabil Eng*. 2013;**21**:265-74. doi.org/10.1109/TNSRE.2012.2218287. PubMed PMID: 23033332.
21. Katsis CD, Exarchos TP, Papaloukas C, Goletsis Y, Fotiadis DI, Sarmas I. A two-stage method for MUAP classification based on EMG decomposition. *Comput Biol Med*. 2007;**37**:1232-40. doi.org/10.1016/j.compbiomed.2006.11.010. PubMed PMID: 17208215.
22. Gerber A, Studer RM, de Figueiredo RJ, Moschytz GS. A new framework and computer program for quantitative EMG signal analysis. *IEEE Trans Biomed Eng*. 1984;**31**:857-63. doi.org/10.1109/TBME.1984.325248. PubMed PMID: 6549305.
23. Loudon GH, Jones NB, Sehmi AS. New signal processing techniques for the decomposition of EMG signals. *Med Biol Eng Comput*. 1992;**30**:591-9. doi.org/10.1007/BF02446790. PubMed PMID: 1297013.
24. Stalberg E, Andreassen S, Falck B, Lang H, Rosenfalck A, Trojaborg W. Quantitative analysis of individual motor unit potentials: a proposition for standardized terminology and criteria for measurement. *J Clin Neurophysiol*. 1986;**3**:313-48. doi.org/10.1097/00004691-198610000-00003. PubMed PMID: 3332279.
25. Florestal JR, Mathieu PA, Malanda A. Automated decomposition of intramuscular electromyographic signals. *IEEE Trans Biomed Eng*. 2006;**53**:832-9. doi.org/10.1109/TBME.2005.863893. PubMed PMID: 16686405.
26. Stashuk D, de Bruin H. Automatic decomposition of selective needle-detected myoelectric signals. *IEEE Trans Biomed Eng*. 1988;**35**:1-10. doi.org/10.1109/10.1330. PubMed PMID: 3338806.
27. Florestal JR, Mathieu PA, McGill KC. Automatic decomposition of multichannel intramuscular EMG signals. *J Electromyogr Kinesiol*. 2009;**19**:1-9. doi.org/10.1016/j.jelekin.2007.04.001. PubMed PMID: 17513128.
28. Zennaro D, Läubli T, Wellig P, Krebs D, Schnoz M, Klipstein A, et al. A method to test reliability and accuracy of the decomposition of multi-channel long-term intramuscular EMG signal recordings. *International journal of industrial ergonomics*. 2002;**30**:211-24. doi.org/10.1016/S0169-8141(02)00126-9.
29. Zennaro D, Wellig P, Koch VM, Moschytz GS, Laubli T. A software package for the decomposition of long-term multichannel EMG signals using wavelet coefficients. *IEEE Trans Biomed Eng*. 2003;**50**:58-69. doi.org/10.1109/TBME.2002.807321. PubMed PMID: 12617525.
30. Wellig P, Moschytz GS, editors. Analysis of wavelet features for myoelectric signal classification. Electronics, Circuits and Systems, 1998 IEEE International Conference on; 1998: IEEE. doi.org/10.1109/icecs.1998.813946.
31. Yamada R, Ushiba J, Tomita Y, Masakado Y, editors. Decomposition of electromyographic signal by principal component analysis of wavelet coefficients. Biomedical Engineering, 2003. IEEE EMBS Asian-Pacific Conference on; 2003: IEEE. doi.org/10.1109/apbme.2003.1302612.
32. Ren X, Huang H, Deng L, editors. MUAP Classification Based on Wavelet Packet and Fuzzy Clus-

tering Technique. Bioinformatics and Biomedical Engineering, 2009. ICBBE 2009. 3rd International Conference on; 2009: IEEE. doi.org/10.1109/icbbe.2009.5163091.

33. Rasheed S, Stashuk DW, Kamel MS. A hybrid classifier fusion approach for motor unit potential classification during EMG signal decomposition. *IEEE Trans Biomed Eng*. 2007;**54**:1715-21. doi.org/10.1109/TBME.2007.892922. PubMed PMID: 17867366.
34. Li D, Pedrycz W, Pizzi NJ. Fuzzy wavelet packet based feature extraction method and its application to biomedical signal classification. *IEEE Trans Biomed Eng*. 2005;**52**:1132-9. doi.org/10.1109/TBME.2005.848377. PubMed PMID: 15977743.
35. LeFever RS, De Luca CJ. A procedure for decomposing the myoelectric signal into its constituent action potentials--Part I: Technique, theory, and implementation. *IEEE Trans Biomed Eng*. 1982;**29**:149-57. doi.org/10.1109/TBME.1982.324881. PubMed PMID: 7084948.
36. Etawil H, Stashuk D. Resolving superimposed motor unit action potentials. *Med Biol Eng Comput*. 1996;**34**:33-40. doi.org/10.1007/BF02637020. PubMed PMID: 8857310.
37. De Figueiredo R, Gerber A. Separation of superimposed signals by a cross-correlation method. Acoustics, Speech and Signal Processing, IEEE Transactions on. 1983;31:1084-9. doi.org/10.1109/TASSP.1983.1164215.
38. Hamid Nawab S, Wotiz R, De Luca CJ. Improved resolution of pulse superpositions in a knowledge-based system EMG decomposition. *Conf Proc IEEE Eng Med Biol Soc*. 2004;**1**:69-71. doi.org/10.1109/iembs.2004.1403092. PubMed PMID: 17271605.
39. Marateb HR, McGill KC. Resolving superimposed MUAPs using particle swarm optimization. *IEEE Trans Biomed Eng*. 2009;**56**:916-9. doi.org/10.1109/TBME.2008.2005953. PubMed PMID: 19272923. PubMed PMCID: 2673334.
40. Florestal JR, Mathieu PA, Plamondon R. A genetic algorithm for the resolution of superimposed motor unit action potentials. *IEEE Trans Biomed Eng*. 2007;**54**:2163-71. doi.org/10.1109/TBME.2007.894977. PubMed PMID: 18075032.
41. Hamilton-Wright A, Stashuk DW. Physiologically based simulation of clinical EMG signals. *IEEE Trans Biomed Eng*. 2005;**52**:171-83. doi.org/10.1109/TBME.2004.840501. PubMed PMID: 15709654.
42. Person K. On Lines and Planes of Closest Fit to System of Points in Space. Philiosophical Magazine, 2; 1901. p. 559-572..
43. Abdi H, Williams LJ. Principal component analysis. Wiley Interdisciplinary Reviews: Computational Statistics. 2010;2:433-59. doi.org/10.1002/wics.101.